ADVANCED FUNCTIONAL MATERIALS
www.afm-journal.de

Materials Views
www.MaterialsViews.com

Diameter Effect on the Sidewall Functionalization of Single-Walled Carbon Nanotubes by Addition of Dichlorocarbene

Kang Zhang, Qing Zhang, Cao Liu, Nicola Marzari, and Francesco Stellacci*

Dichlorocarbene is added to the sidewalls of single-walled carbon nanotubes (SWNTs) with diameters ranging from 1.2 to 2.2 nm. Small diameter SWNTs are found to react much more easily than large diameter SWNTs. Upon functionalization, the conductance could be largely preserved for almost all SWNTs, while an effective bandgap increase for functionalized metallic SWNTs (m-SWNTs) and a bandgap reduction for functionalized semiconducting SWNTs (s-SWNTs) are generally observed. The results suggest that [2 + 1] cycloaddition is an excellent choice of processing, resulting in SWNTs over a large diameter range with electronic properties that are almost unaffected. Furthermore, possible separation of SWNTs according to their diameters could be achieved due to the apparent diameter-dependent reactivity.

1. Introduction

Covalent sidewall functionalization has been proven to be one of the promising methods to modify the properties of single-walled carbon nanotubes (SWNTs) for many applications, such as increasing the solubility of SWNTs, improving the performance of SWNT electronic devices and separation of SWNTs by their electronic types.[1–3,29] As an important type of covalent functionalization, [2 + 1] cycloaddition of SWNTs has been extensively studied theoretically.[4–12] Recently, a remarkable conductance preservation effect has been experimentally observed upon [2 + 1] cycloadditions of SWNTs.[13] The conductance preservation effect has been attributed to the bond cleaving between adjacent sidewall carbon atoms, leading to sp^2 hybridizations in sharp contrast with most types of covalent functionalization where sp^3 hybridizations are formed.[7,13]

Since SWNT sidewall bond cleaving is expected to be a curvature induced effect, the conductance preservation effect by the sidewall C−C bond cleaving should vary with the SWNT diameter and chirality.[5,7] Actually, Lee and Marzari predicted that the sidewall bond cleaving could be favorable for armchair SWNTs up to a diameter of 2.4 nm by [2 + 1] cycloaddition.[7] Lopez-Bezanilla et al. predicted that zigzag SWNTs with diameters larger than 1.5 nm would not exhibit sidewall bond cleaving by [2 + 1] cycloaddition of CH_2 groups and thus significant reduction of the conductance should be observed.[5]

Furthermore, the chemical reactivity of SWNTs is also expected to vary with diameter, chirality and electronic type, as suggested by many theoretical studies.[12,15–17,35] Haddon et al. predicted that the strain in SWNT arose from a combination of π-orbital misalignment and pyramidalization, and an increase in SWNT reactivity was expected with increasing strain.[17] Chen et al. showed that π-orbital misalignment and pyramidalization scaled inversely with SWNT diameter and predicted a sidewall opening by chemical modification.[11,35] Li et al. constructed a unique curvature parameter *K*, which was defined as the average curvature of the corresponding arc of a C−C bond in the SWNT, and then they showed that, only for the zigzag tubes with smaller *K*, the cycloaddition of dichlorocarbene on any C−C bonds led to the adducts with three-membered ring structure (sidewall C−C bond closed structure).[12] In summary, all these theoretical studies support that curvature induced strain is the major cause of the reactivity of SWNTs. Thus, smaller diameter SWNTs are generally expected to be more reactive.[12,15–17] In fact, for the case of solution-phase ozonolysis, Banerjee et al. showed that smaller diameter SWNTs reacted much more extensively than large diameter SWNTs for a diameter range of 0.7–1.2 nm HiPco SWNTs.[18] However, no experimental results have been reported, to the best of our knowledge, on the diameter dependent reactivity for [2 + 1] cycloadditions.

If the reactivity is determined by the curvature of SWNT sidewall carbon bonds, [2 + 1] functionalization could have a potential application in separating SWNTs according to their diameters. More importantly, for pristine SWNTs with a narrow diameter distribution, one could even use [2 + 1] functionalization to separate SWNTs according to their chirality or circumferential angle, leading a possible way towards monodisperse SWNTs. In addition, the great conductance preserving effect suggests that [2 + 1] cycloaddition is a promising treatment to assist the handling and processing of SWNTs for electronic devices. Furthermore, the robustness of the covalent functionalization, the almost unaffected excellent electrical property and

K. Zhang, Prof. Q. Zhang, C. Liu
School of Electrical & Electronic Engineering
Nanyang Technological University
639798 Singapore, Singapore
E-mail: eqzhang@ntu.edu.sg
K. Zhang, Prof. Q. Zhang, C. Liu
Advanced Materials for Micro- and Nano-Systems
Singapore–MIT Alliance
National University of Singapore
4 Engineering Drive 3, Singapore 117576, Singapore
Prof. N. Marzari, Prof F. Stellacci
Department of Materials Science and Engineering
Ecole Polytechnique Fédérale de Lausanne
CH-1015 Lausanne, Switzerland

DOI: 10.1002/adfm.201201777

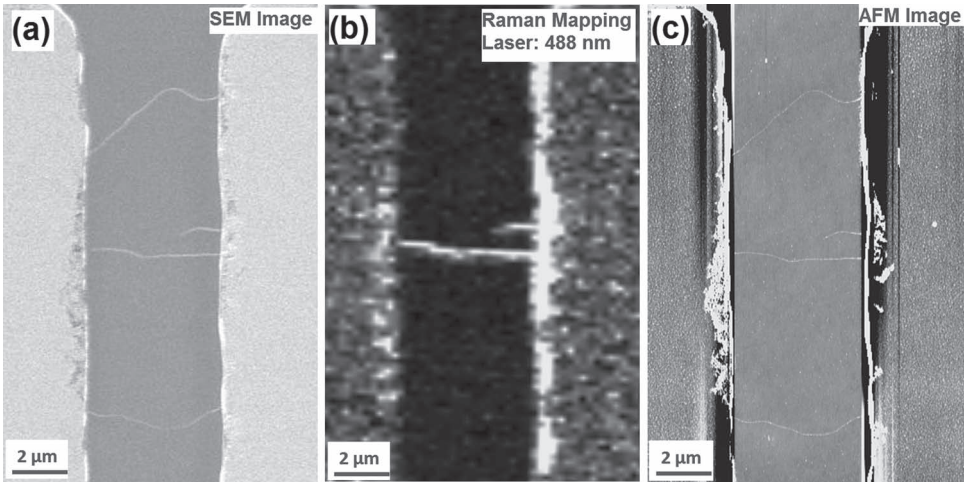

Figure 1. A typical structure under functionalization: a) SEM image, b) Raman mapping of the structure shown in (a) with G band (1500–1600 cm^{-1}) peak intensity under 488 nm excitation, and c) AFM image of the structure shown in (a).

the high surface to volume ratio of SWNTs suggest that [2 + 1] cycloaddition functionalized SWNTs have great potentials to be used as sensing elements.

In this work, as-grown individual SWNTs with diameters ranging from 1.2 to 2.2 nm are studied in terms of their reactivity and electrical properties upon dichlorocarbene [2 + 1] cycloaddition. Raman spectroscopy is used to characterize the diameter dependent effect on the functionalization. Electrical measurements are also performed on simple field-effect transistor (FET) structures before and after a significant degree of the functionalization. Our results show that small diameter SWNTs react much more easily than large diameter SWNTs. No detectable difference in the reactivity between m-SWNT and s-SWNT is observed. Furthermore, the conductances of SWNTs are largely preserved with a significant degree of the functionalization. Effective bandgap increase is observed for functionalized m-SWNTs. In contrast, effective bandgap reduction is found for functionalized s-SWNTs.

2. Results and Discussion

2.1. Diameter Effects on Reactivity

Thermal-CVD grown SWNTs on SiO_2 substrates are used for this study. In order to confine the functionalization only to the sidewalls of SWNTs, Ti/Au electrodes with ≈5 μm spacing are used to cover both ends of the SWNTs. **Figure 1**a shows an SEM image of a typical sample before dichlorocarbene functionalization. The electrodes also hold the SWNTs during the reaction and, at the same time, serve as markers to locate SWNTs.

Raman scattering is performed with different excitation lines (488, 532, and 633 nm) to characterize the SWNTs before and after the functionalization. The Raman spectrum for a SWNT has three distinct modes, i.e. the radial breathing mode (RBM), D mode and G mode. RBM band is usually in the range of 100–300 cm^{-1}, arising from the photon scattering caused by symmetric in-phase displacements of all the carbon atoms in the SWNT in the radial direction and, hence, is used to determine the SWNT diameter.[21] The electronic type of a SWNT can also be determined by examining the RBM bands with the excitation laser wavelength.[21,33] The G band around 1500–1600 cm^{-1} associates with the tangential vibrational modes of SWNTs while the D band around 1300–1400 cm^{-1} refers to symmetry-breaking perturbation on the hexagonal sp^2 bonded carbon atoms.[21]

Figure 1b shows the Raman G band mapping on the sample. The thickening of the SWNT image in the mapping is caused by a low space resolution of ≈1 μm of the Raman spectroscopy. It is noted from Figure 1b that not all the SWNTs in the SEM image (Figure 1a) show in the Raman mapping image. Only those SWNTs in good resonance with the incident excitation lasers (532 nm in Figure 1b) as well as in the direction of the polarization of the excitation laser can be observed.[21] Furthermore, even for some SWNTs in good resonance with the incident laser, only about 1/5 of them (estimated from our measurements with SWNT diameter distribution of 1.2–2.2 nm) have their RBM bands detected. For comparison, the AFM image of the sample is shown in Figure 1c.

In the literature, the RBM band intensity reduction and the D band to G band intensity ratio increase are usually used as the evidence of successful covalent functionalization.[19–22,25] However, in our experiment, the D/G ratio increase is found to be more reliable than the RBM intensity decrease as the covalent functionalization indicator, probably because RBM intensity is sensitive to the local environment of the SWNT.[23,34] Furthermore, it has been pointed out that the D/G ratio indicator works well only at low degrees of functionalization.[25] For high degrees of functionalization, the SWNTs are likely out of resonance with the excitation laser as their electronic structures are largely damaged.[25] Therefore, in order to avoid large damage by high degree functionalization, we have kept the degree of dichlorocarbene functionalization to be low.

Two typical Raman spectra for a thin and thick SWNT are compared in **Figure 2**. In this figure, the low wavenumber

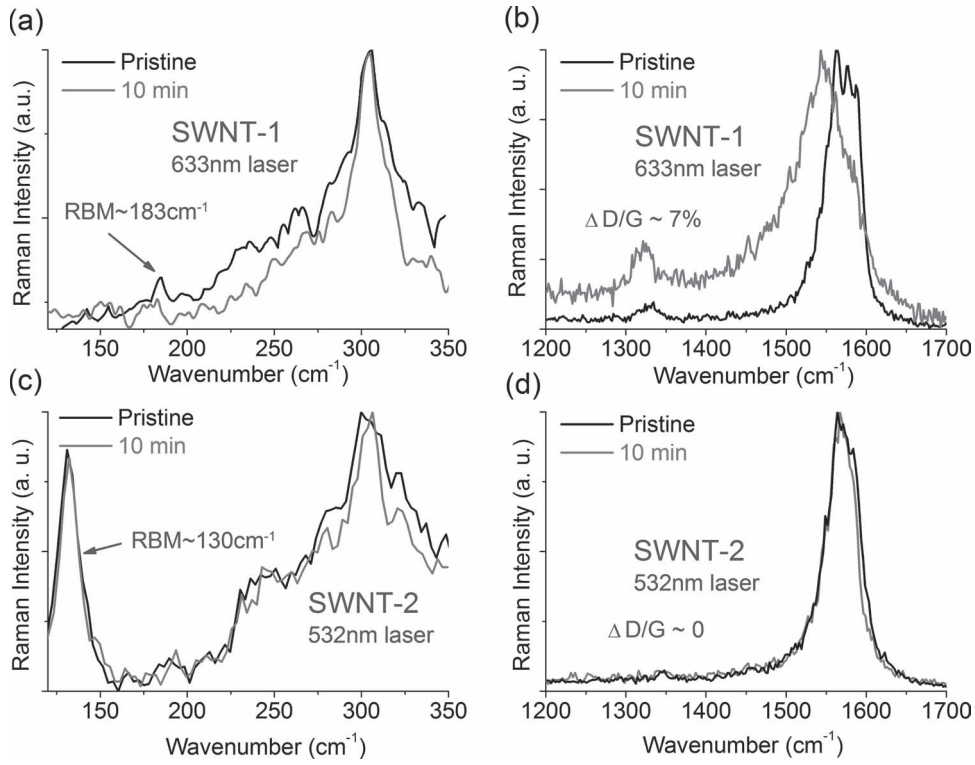

Figure 2. Raman spectra comparison of SWNT-1 and SWNT-2 before and after the functionalization. a) RBM band comparison of SWNT-1. b) D/G ratio comparison of SWNT-1. c) RBM band comparison of SWNT-2. d) D/G ratio comparison of SWNT-2.

region showing RBM band is normalized to the silicon peak at ≈303 cm^{-1}, while the high wavenumber region is normalized to the G band peak ≈1550–1600 cm^{-1}. Figure 2a shows a RBM band feature of ≈183 cm^{-1} with 633 nm excitation, which corresponds to an m-SWNT (SWNT-1) with diameter of ≈1.36 nm determined with the aid of Kataura plots.[21,33] Similarly, the ≈130 cm^{-1} RBM feature in Figure 2c with 532 nm excitation could be used to assign this SWNT to a ≈1.91 nm diameter m-SWNT (SWNT-2). From Figures 2b, a sharp increase in the D band intensity for SWNT-1 after the functionalization suggests that significant number of dichlorocarbene groups have covalently attached to the sidewall of SWNT-1 after only 10 min functionalization. In contrast, no detectable change in the D/G ratio is observed for SWNT-2 after 10 min functionalization as shown in Figure 2d.

Figures 3 shows another set of comparison of two s-SWNTs with diameters of ≈1.25 nm (SWNT-3) and ≈2.2 nm (SWNT-4) respectively. Again a sharp contrast can be found in the variation in the D/G intensity ratio (see Figure 3b,d), suggesting that the small s-SWNT is more reactive than the large one.

It can be seen that, in Figure 2b and Figure 3b, before the reaction, the SWNTs have some defects, which may affect the reactivity. However, our experimental results show that the existing defects do not contribute significantly on the reactivity in the functionalization probably due to the extremely high reactivity of dichlorocarbene species and the high energy release by addition of dichlorocarbene. In this sense, the strain energy release is considered to be the major driving force in this reaction so that the functionalization could occur easily at defect-free C–C bonds, while the defects do not play a significant role.

If the small diameter SWNTs have a high degree of functionalization, their G bands resonance should also largely decrease as the loss in resonance with the excitation laser.[25] This can also be evidenced by our experiments. **Figure 4** shows a set of Raman spectra comparison in between four SWNTs (SWNT-5 to SWNT-8). Each of the spectra is normalized to silicon (their substrates) peaks ≈520 cm^{-1} and then rescaled to arbitrary unit. It is clearly shown that the small diameter SWNTs in Figure 4a,b show a large decrease in their G band intensities after the functionalization. While for the large diameter SWNTs in Figure 4c,d, the G band intensities only slightly drop.

In order to further confirm the diameter effect on reactivity, more experiments are performed on a thick SWNT network with diameter from 0.9 to 1.6 nm, and the Raman scattering results further confirm that small diameter SWNTs react much more extensively than those large diameter SWNTs (see Supporting Information).

Theoretically, even with the same diameter, different chirality SWNTs will have different strain energies.[12,15–17] The maximum difference in the circumferential angle is 30° for the sidewall bonds.[12] Thus it is generally expected, for example, that 1.5 nm diameter SWNTs with large circumferential angles might react slower than 1.6 nm diameter SWNTs with small circumferential angles, but they should always react faster than all those 1.9 nm SWNTs. However, as lack of precise measurements on the degree of functionalization, we are not able to draw a clear conclusion from our observations at this moment.

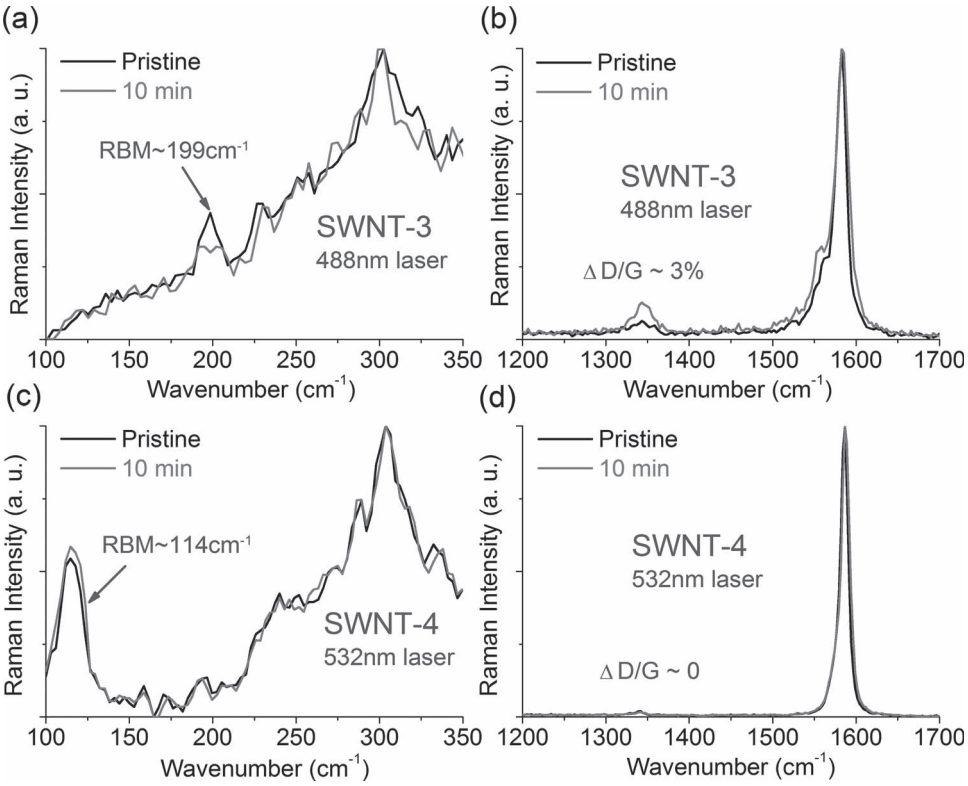

Figure 3. Raman spectra comparison of SWNT-3 and SWNT-4 before and after the functionalization. a) RBM band comparison of SWNT-3. b) D/G ratio comparison of SWNT-3. c) RBM band comparison of SWNT-4. d) D/G ratio comparison of SWNT-4.

From comparison, we see that small diameter SWNTs generally react much more easily than large diameter SWNTs. The curvature induced strains on the sidewall carbon bonds are suggested to be a main driving force for such functionalization reaction. In addition, we have not observed a significant difference in the reactivity between m-SWNTs and s-SWNTs, while several groups did observe the difference in many other types of functionalization.[26–29,32]

2.2. Diameter Effects on Electrical Performance

Electrical characterization before and after the functionalization is performed on individual SWNTs on a typical FET platform (see details in Experimental Section) where a heavily doped p-type Si is used as the back gate and Ti/Au electrodes are used as source (S) and drain (D), respectively. **Figure 5**a shows an AFM image of a SWNT whose two ends are covered by the S and D electrodes. The remaining ≈5 μm portion in the middle serves as the channel and is exposed to the functionalization. The Raman mapping image of the sample is shown in Figure 5b.

It is worth noting here that the contact resistance may vary after the functionalization depending on the physical contact properties between the SWNTs and electrodes. In order to avoid the problem, those SWNTs for FET fabrication are generally chosen to be > ≈100 μm in length and the length of the SWNTs under the source and drain are controlled to be > ≈40 μm. The large interface area under the electrodes is thus unaffected during the reactions. We also perform control experiment with the contacts covered with thick silicon nitride and find that there is no difference between the covered and uncovered SWNT FETs. This confirms that the functionalization does not affect the contact resistance. Therefore, in this paper, all results are taken from SWNT FETs with contacts uncovered in order to eliminate contaminations introduced by the additional silicon nitride deposition and lift-off processes.

2.2.1. Response of m-SWNT

According to our observations, most of m-SWNTs have weak gate dependence. This could be due to the curvature induced tiny bandgap of a general chiral m-SWNT (non-armchair m-SWNT).[30] In this study, two m-SWNTs with diameter ≈1.38 nm and ≈1.88 nm are examined in terms of their electrical response to the functionalization. The degree of the functionalization is roughly controlled by adjusting the reaction time. We find that 10 min functionalization of SWNT-A and 30 min functionalization of SWNT-B can cause a comparable significant increase in the D/G intensity ratio of the two tubes (**Figure 6**b,e).

From Figure 6c,f, one can see that the on-state conductances for both m-SWNTs decrease by less than 50%, indicating that diameter has little influence on the conductivity preservation effect upon dichlorocarbene functionalization. However, it is also noticed that, for both m-SWNTs, the on off ratios increase

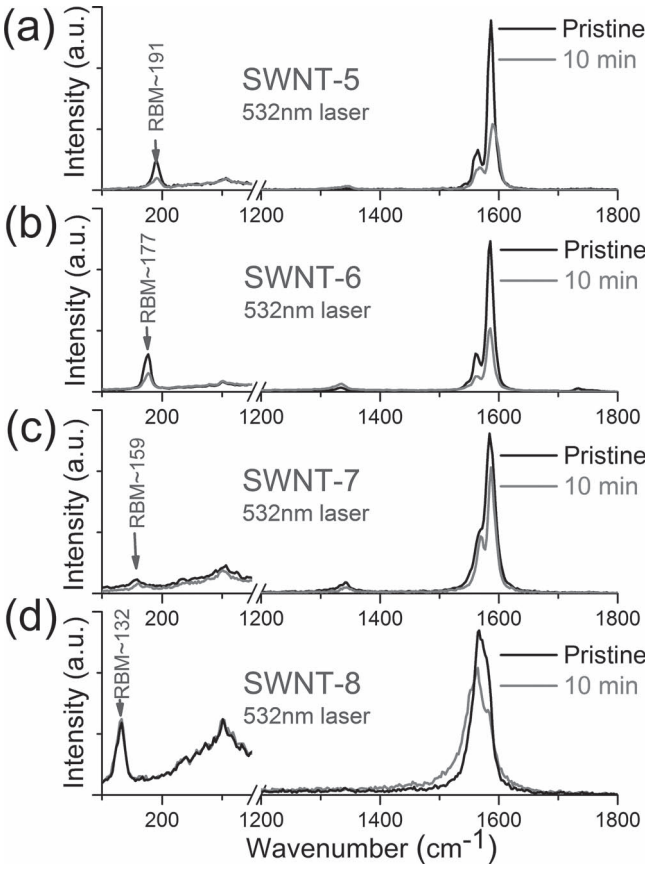

Figure 4. Raman G band intensity comparison of SWNTs with different diameter before and after the functionalization under 532 nm laser excitation. a) Raman intensity comparison of SWNT-5 (RBM ≈ 191 cm^{-1}). b) Raman intensity comparison of SWNT-6 (RBM ≈ 177 cm^{-1}). c) Raman intensity comparison of SWNT-7 (RBM ≈ 159 cm^{-1}). d) Raman intensity comparison of SWNT-8 (RBM ≈ 132 cm^{-1}).

from ≈1.5 to ≈5, suggesting that there is an effective bandgap opening of m-SWNTs by adding dichlorocarbene to their sidewalls. To the best of our knowledge, this is the first report on dichlorocarbene addition induced bandgap opening in m-SWNT observed in electrical measurements. This is consistent with the observation by Kamaras et al., where a dramatic decrease of

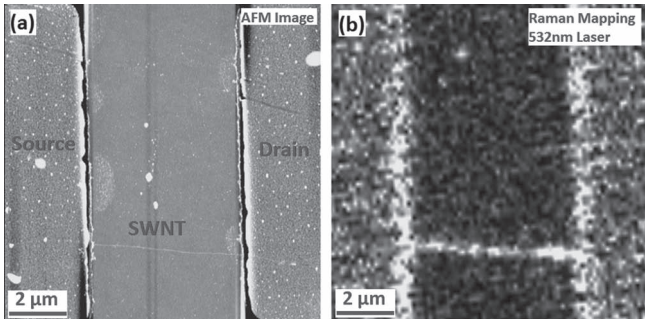

Figure 5. AFM image and Raman mapping of a typical structure used for electrical measurement. a) AFM image with source, drain, and SWNT channel labeled. b) Raman mapping of the structure in (a) with G band (1500–1600 cm^{-1}) peak intensity under 532 nm excitation.

absorption in the far-infrared (FIR) region on dichlorocarbene functionalized SWNTs was observed in solution phase which could also be attributed to an effective bandgap opening.[31]

2.2.2. Response of s-SWNTs

Figure 7 shows the electrical measurements and Raman scattering results of two s-SWNTs with diameters of ≈1.31 nm and ≈1.69 nm, respectively. Similarly, SWNT-C is subjected to a 10 min reaction while the SWNT-D is for a 30 min reaction. Raman scattering results (Figure 7b,e) provide with clear evidence of successful functionalizations for both SWNTs.

From the electrical results shown in Figure 7f for SWNT-D, one can find that the on-state conductance drops by ≈70%, slightly higher than the case of the m-SWNTs (SWNT-A and SWNT–B). However, for SWNT-C (≈1.31 nm diameter) shown in Figure 7c, the on-state conductance does not drop significantly even after a significant degree of the functionalization (see Raman results in Figure 7a,b).

It is also important to note from the electrical results that both s-SWNTs exhibit an apparent decrease in their on/off ratios, implying effective bandgap reduction. This is probably due to the quasi-bound states formed within the original bandgap which could effectively reduce the bandgap as proposed by Cho et al. with their calculations.[14] However, the bandgap reduction and conductance reduction are not as significant as observed in previous work.[13]

In above FET devices, the degree of functionalization is estimated to be ≈2–5% by inspecting the change in the D/G ratio and the decrease of G band intensity in the Raman spectra.[29] In our experiment, the conductance drop is founded to be insensitive to the degree of functionalization. However, in order to make a reasonable comparison, we manage to achieve similar degree of functionalization in above FET devices through controlling the reaction time.

As the conductance preserving effect can be attributed to the sidewall C−C bonding cleaving, the attached functional groups on the [2 + 1] cycloaddition should not have significant effect on the conductance of the SWNT (except that certain chemical groups have strong electron donating/withdrawing effect or certain chemical groups interact with the SWNT). As a comparison, we also perform the well-established Bingel reaction to introduce $(COOEt)_2C$: functional groups instead of dichlorocarbene to SWNT sidewall and similar electronic property changes is observed.[36]

3. Conclusions

Our experimental evidence confirms that SWNTs with small diameter are functionalized with [2 + 1] cycloaddition of dichlorocarbene groups much more easily than large diameter SWNTs, regardless semiconducting or metallic SWNTs. The on-state conductance could be largely preserved over a broad diameter distribution upon a significant degree of functionalization. Effective bandgap variations are generally observed for all SWNTs under investigation. We suggest that [2 + 1] cycloadditions are suitable for SWNT functionalization over a large diameter range with their conductivities largely preserved.

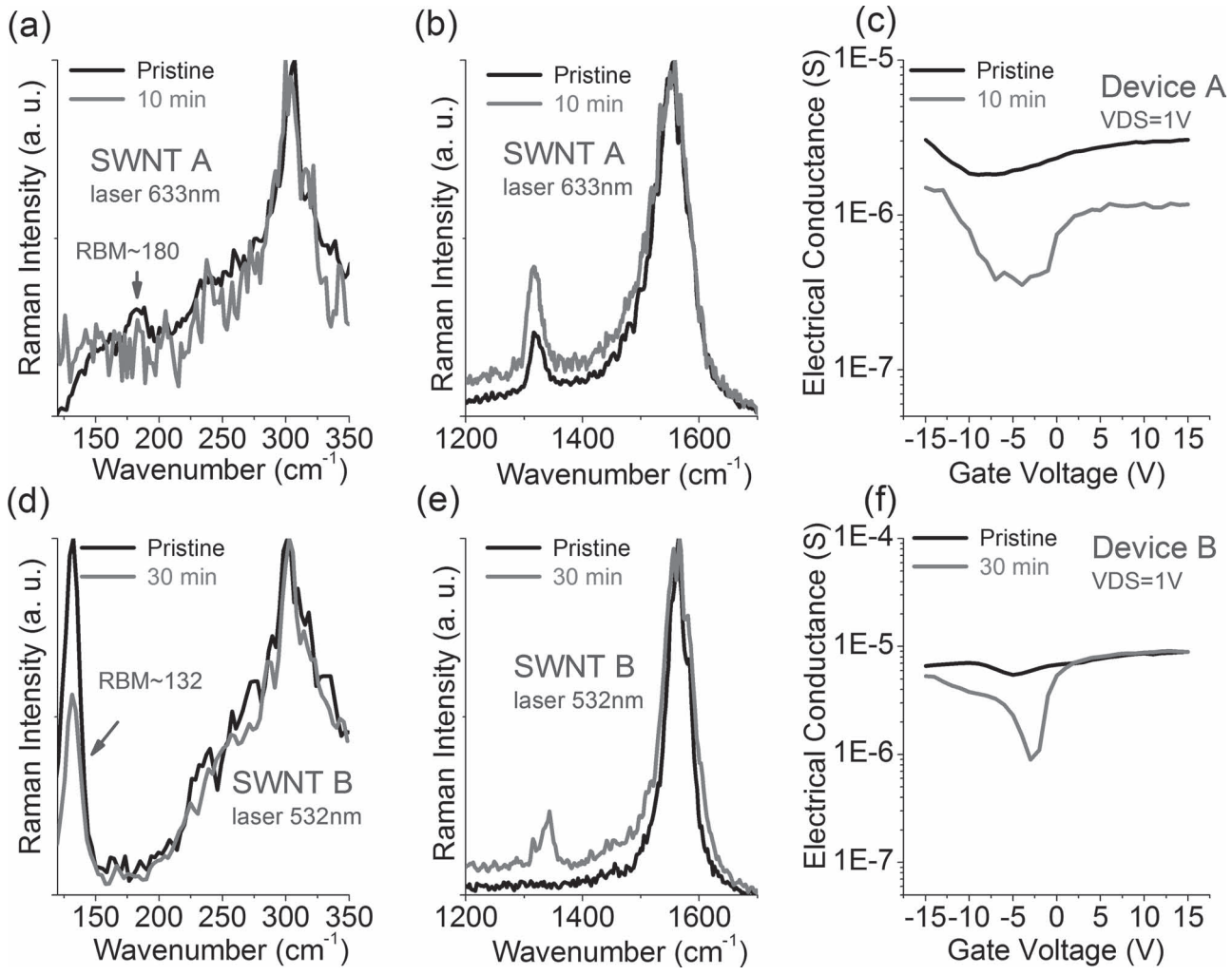

Figure 6. Raman spectra and electrical response comparisons of two m-SWNTs with different diameters before and after the functionalization. a) RBM band comparison of SWNT-A. b) D/G ratio comparison of SWNT-A. c) Electrical response comparison of SWNT-A. d) RBM band comparison of SWNT-B. e) D/G ratio comparison of SWNT-B. f) Electrical response comparison of SWNT-B.

4. Experimental Section

Sample Preparation for Reactivity Comparison: Nearly isolated SWNTs were grown using thermal CVD with ferritin-based catalysts at 925 °C on heavily doped p-silicon substrate capped with 500 nm SiO_2. These as-grown SWNTs were then covered by Ti/Au electrodes with 5 μm spacing using standard metallization and photolithography techniques. SEM (LEO 1550 Gemini), AFM (Cypher AFM, Asylum Research) and Raman scattering (WITec) with different excitation laser lines (488, 532, and 633 nm) were performed. SWNTs showing both RBM band and G-band were selected for further functionalization reaction.

Sample Preparation for Electrical Measurements: Largely separated SWNTs were grown by thermal-CVD with ferritin catalyst at 925 °C on heavily doped p-silicon substrate capped with 500 nm SiO_2 and with fine SiO_2 markers, which were observable under an optical microscope. Raman mapping was then performed according to the SEM images to locate the desired SWNTs. The selected SWNT then had both ends covered with Ti/Au electrodes using standard metallization and photolithography techniques. The heavily doped p-type Si substrate served as the back gate, while the electrodes served as the source and drain. Electrical measurements were performed before and after the functionalization.

Chemical Synthesis: A typical 10 min reaction involved immersing the as-prepared samples into a well-stirred, highly basic solution of potassium *tert*-butoxide (1 g, ≥97%, Sigma-Aldrich) dissolved in 10 mL tetrahydrofuran (10 mL, ≥99.9%, Sigma-Aldrich) in the presence of phase transfer catalyst (5 mg, Dowex 1 × 2 chloride form, Sigma-Aldrich). Chloroform (1.5 mL, ≥99.8%, Sigma-Aldrich) was then added dropwise to the mixture in an inert gas environment. The samples were then rinsed thoroughly with acetone, isopropyl alcohol, and deionized water and then heated at 100 °C for 5 min on a hot plate to remove chemical residuals before Raman spectroscopy and electrical measurements.

Raman Spectroscopy Characterization: Raman measurements were performed with excitation laser lines of 488, 532, and 633 nm using a confocal Raman system (WITec) in air ambient with the Raman emission collected by a 100× objective lens. Raman excitation laser intensity was kept sufficiently low to eliminate any possible damage to the SWNTs. Raman mappings for each sample were performed in one orientation to avoid any polarization effect.

Supporting Information

Supporting Information is available from the Wiley Online Library or from the author.

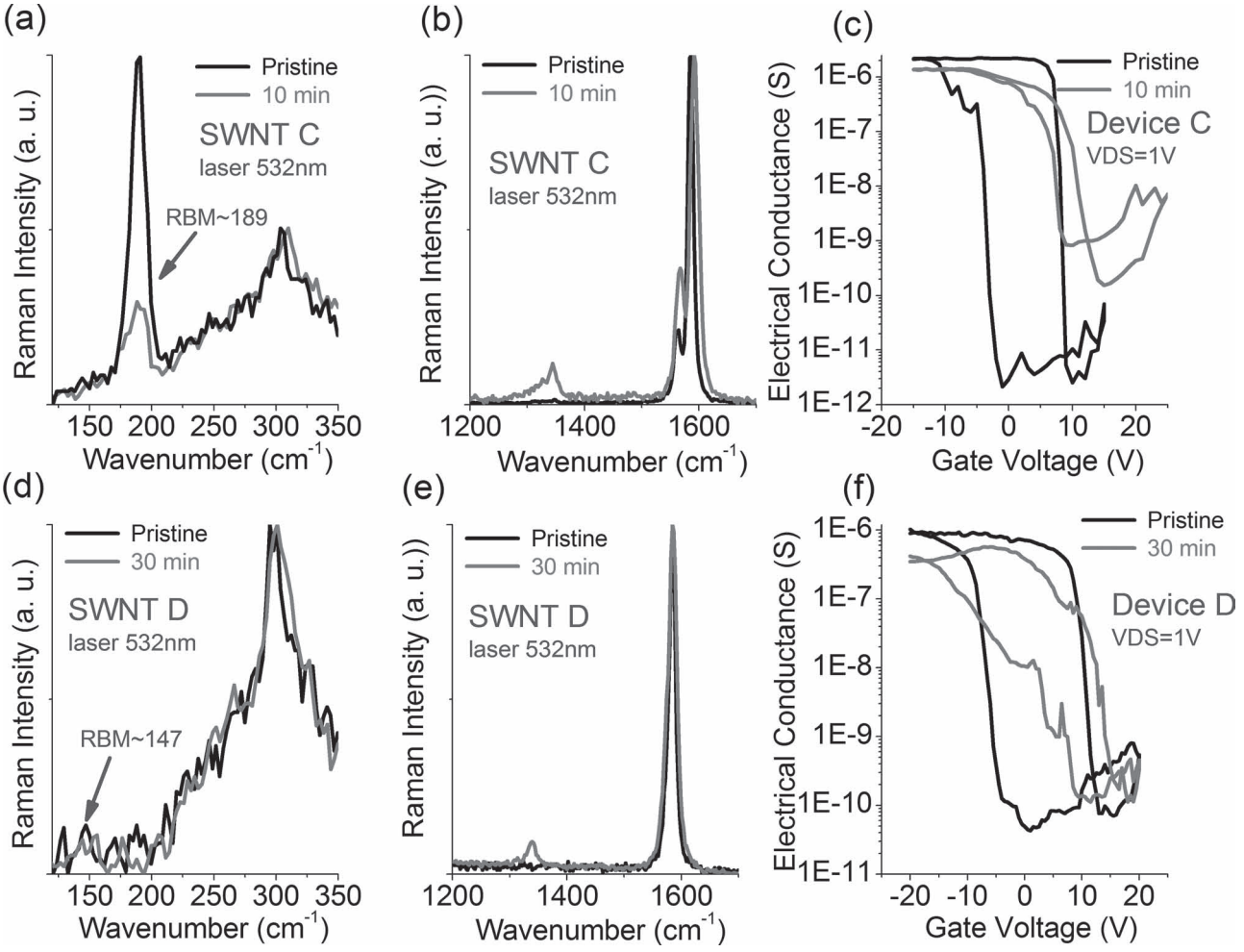

Figure 7. Raman spectra and electrical response comparisons of two s-SWNTs with different diameter before and after the functionalization. a) RBM band comparison of SWNT-C. b) D/G ratio comparison of SWNT-C. c) Electrical response comparison of SWNT-C. d) RBM band comparison of SWNT-D. e) D/G ratio comparison of SWNT-D. f) Electrical response comparison of SWNT-D.

Acknowledgements

This work was supported in part by Singapore-MIT Alliance. The authors would like to thank their colleagues at the School of Electrical & Electronic Engineering, Nanyang Technological University for valuable discussions.

Received: June 29, 2012
Published online: August 3, 2012

[1] A. Hirsch, *Angew. Chem. Int. Ed.* **2002**, *41*, 1853.
[2] S. Banerjee, M. G. C. Kahn, S. S. Wong, *Chem. Eur. J.* **2003**, *9*, 1899.
[3] S. Campidelli, M. Meneghetti, M. Prato, *Small* **2007**, *3*, 1672.
[4] E. Y. Li, N. Poilvert, N. Marzari, *ACS Nano* **2011**, *5*, 4455.
[5] A. Lopez-Bezanilla, X. Blase, S. Roche, *Nano Res.* **2010**, *3*, 288.
[6] H. Park, J. J. Zhao, J. P. Lu, *Nano Lett.* **2006**, *6*, 916.
[7] Y.-S. Lee, N. Marzari, *Phys. Rev. Lett.* **2006**, *97*, 116801.
[8] E. Cho, H. Kim, C. Kim, S. Han, *Chem. Phys. Lett.* **2006**, *419*, 134.
[9] H. F. Bettinger, *Chem. Eur. J.* **2006**, *12*, 4372.
[10] J. J. Zhao, Z. F. Chen, Z. Zhou, H. Park, P. V. Schleyer, J. P. Lu, *ChemPhysChem* **2005**, *6*, 598.
[11] Z. F. Chen, S. Nagase, A. Hirsch, R. C. Haddon, W. Thiel, P. V. Schleyer, *Angew. Chem. Int. Ed.* **2004**, *43*, 1552.
[12] J. Q. Li, G. X. Jia, Y. F. Zhang, Y. Chen, *Chem. Mater.* **2006**, *18*, 3579.
[13] C. Liu, Q. Zhang, F. Stellacci, N. Marzari, L. X. Zheng, Z. Y. Zhan, *Small* **2011**, *7*, 1257.
[14] E. Cho, H. Kim, C. Kim, S. Han, *Chem. Phys. Lett.* **2006**, *419*, 134.
[15] K. Seo, K. A. Park, C. Kim, S. Han, B. Kim, Y. H. Lee, *J. Am. Chem. Soc.* **2005**, *127*, 15724.
[16] S. Banerjee, T. Hemraj-Benny, S. S. Wong, *Adv. Mater.* **2005**, *17*, 17.
[17] M. A. Hamon, M. E. Itkis, S. Niyogi, T. Alvaraez, C. Kuper, M. Menon, R. C. Haddon, *J. Am. Chem. Soc.* **2001**, *123*, 11292.
[18] S. Banerjee, S. S. Wong, *Nano Lett.* **2004**, *4*, 1445.
[19] M. S. Dresselhaus, A. Jorio, A. G. Souza, R. Saito, *Phil. Trans. R. Soc. A* **2010**, *368*, 5355.
[20] A. G. Souza, A. Jorio, G. G. Samsonidze, G. Dresselhaus, R. Saito, M. S. Dresselhaus, *Nanotechnology* **2003**, *14*, 1130.
[21] M. S. Dresselhaus, G. Dresselhaus, A. Jorio, *J. Phys. Chem. C* **2007**, *111*, 17887.

[22] A. Jorio, C. Fantini, M. A. Pimenta, R. B. Capaz, G. G. Samsonidze, G. Dresselhaus, M. S. Dresselhaus, J. Jiang, N. Kobayashi, A. Gruneis, R. Saito, *Phys. Rev. B* **2005**, 71.
[23] P. T. Araujo, P. B. C. Pesce, M. S. Dresselhaus, K. Sato, R. Saito, A. Jorio, *Physica E* **2010**, *42*, 1251.
[24] S. D. M. Brown, A. Jorio, P. Corio, M. S. Dresselhaus, G. Dresselhaus, R. Saito, K. Kneipp, *Phys. Rev. B* **2001**, 63.
[25] R. Graupner, *J. Raman Spectrosc.* **2007**, *38*, 673.
[26] M. S. Strano, C. A. Dyke, M. L. Usrey, P. W. Barone, M. J. Allen, H. W. Shan, C. Kittrell, R. H. Hauge, J. M. Tour, R. E. Smalley, *Science* **2003**, *301*, 1519.
[27] C. J. Wang, Q. Cao, T. Ozel, A. Gaur, J. A. Rogers, M. Shim, *J. Am. Chem. Soc.* **2005**, *127*, 11460.
[28] H. M. So, B. K. Kim, D. W. Park, B. S. Kim, J. J. Kim, K. J. Kong, H. J. Chang, J. O. Lee, *J. Am. Chem. Soc.* **2007**, *129*, 4866.
[29] M. Kanungo, H. Lu, G. G. Malliaras, G. B. Blanchet, *Science* **2009**, *323*, 234.
[30] C. T. White, J. W. Mintmire, *J. Phys. Chem. B* **2005**, *109*, 52.
[31] H. Hu, B. Zhao, M. A. Hamon, K. Kamaras, M. E. Itkis, R. C. Haddon, *J. Am. Chem. Soc.* **2003**, *125*, 14893.
[32] M. K. Bayazit, K. S. Coleman, *J. Am. Chem. Soc.* **2009**, *131*, 10670.
[33] H. Kataura, Y. Kumazawa, Y. Maniwa, I. Umezu, S. Suzuki, Y. Ohtsuka, Y. Achiba, *Synth. Met.* **1999**, *103*, 2555.
[34] M. Steiner, M. Freitag, J. C. Tsang, V. Perebeinos, A. A. Bol, A. V. Failla, P. Avouris, *Appl. Phys. A: Mater. Sci. Process.* **2009**, *96*, 271.
[35] Z. F. Chen, W. Thiel, A. Hirsch, *ChemPhysChem* **2003**, *4*, 93.
[36] K. S. Coleman, S. R. Bailey, S. Fogden, M. L. H. Green, *J. Am. Chem. Soc.* **2003**, *125*, 8722.